X-RAY PRECESSION TECHNIQUES

D. JEROME FISHER, *University of Chicago, Chicago 37, Illinois*

ABSTRACT

Herewith is described a modified technique for taking orientation photos and evaluating them with some precision. Also are discussed for the triclinic case: (1) the identification of non-axial precessing directions; (2) the indexing of non-axial precession photos; and (3) the computation of reciprocal lattice spacings in non-axial directions. The paper concludes with simplified charts for determining the setting of the various layer-line screens.

PRECESSION ORIENTATION PICTURES

Orientation photos of single crystals with the precession camera are 0-level pictures taken by omitting the layer-line screen and using unfiltered radiation. The precessing angle is generally kept small, so that the 0-level Laue streaks are limited to the blank n-level area. The theory and practice of the technique are briefly described in Buerger (1944, 21–27).

X-ray photos herewith are all of the triclinic chalcanthite with copper radiation at $F=6.00$ cms., unless otherwise stated. In all cases the pictures are oriented as they appear in the cassette looking in the direction of travel of the direct beam with the dial axis [c^*] horizontal. Unless otherwise indicated all reproductions are at natural scale. The exposures were unduly long for purposes of illustration.

A correctly-oriented crystal on the precession instrument has a reciprocal translation direction (generally a reciprocal axis) parallel to the dial axis, and a direct-lattice translation direction (generally a crystal axis) as the precessing direction. Such a crystal yields a diffraction pattern (Fig. 29),[1] the central part of which consists of radiating 0-level Laue streaks whose ends lie along the circumference of a circle, the circle of precession. One set of these streaks is horizontal and is parallel to the dial axis; these and the other streaks radiate in the direction of (what would appear on a 0-level precession film as) spots of simple indices. If the precessing angle ($\bar{\mu}$) is not too small, some of the 0-level spots will appear along the streaks; thus in Fig. 29 near the end of the east streak appears the K_β spot for (001)* and along the near-north and near-south streaks (marking [b^*]) are shown both K_α and K_β spots for $(0\bar{1}0)^*$ and (010)* respectively; the K_β spot of the latter is almost cut out by the direct beam-stopping cup.

As the various central lines of nodes of some one 0-level of the reciprocal lattice undergo a precessing motion, they slide or shear over the

[1] The numbers here assigned to figures, tables and formulas are in continuation of those used in the preceding paper (Fisher, 1952 *b*).

base of the calotte which they cut out of the sphere of reflection. While this results in a set of spots which unite into a 0-level cone axis ring as described in the previous paper, they form a series of radiating Laue streaks on the orientation film. In short a precession orientation photograph of a correctly set crystal appears the same as a 0-level precession photograph made at the same $\bar{\mu}$-angle taken with unfiltered radiation,

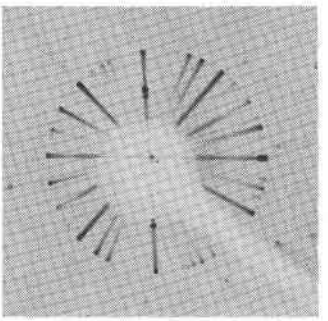

FIG. 29. Central portion of a precession orientation photo of chalcanthite, precessing on [a], $\bar{\mu}=7°$.

except that the former also carries some higher-level diffractions. However, if the crystal is not approximately correctly oriented, any layer line screen present will cut off the ends of some of the 0-level streaks.

ORIENTATION PROCEDURE

In working with a reasonably well-developed subhedron, time will generally be saved if preliminary orientation is obtained with the optical goniometer. If the substance is unknown, one can proceed by standard Goldschmidt methods to locate the crystal axes. If the substance is monoclinic or triclinic, the stereographic technique (Fisher, 1951) is handy for setting a reciprocal axis as the dial axis.

If one is dealing with an unknown anhedron of a non-opaque material, it may be well to obtain optical data on the universal microscope (Fisher, 1952 *c*) to establish the crystal division (and the crystal system if biaxial). For any crystal neither isometric nor triclinic this would set up one or more axial directions. If the anhedron is opaque, one must proceed by trial and error *X*-ray methods of orientation, unless cleavage or some similar "directions" are exhibited.

Having reached the stage where a precession orientation picture showing a Laue streak diffraction pattern outlining a suitable circle of precession has been obtained, the procedure will vary with different situations. A suitable circle of precession may be taken as one which contains enough

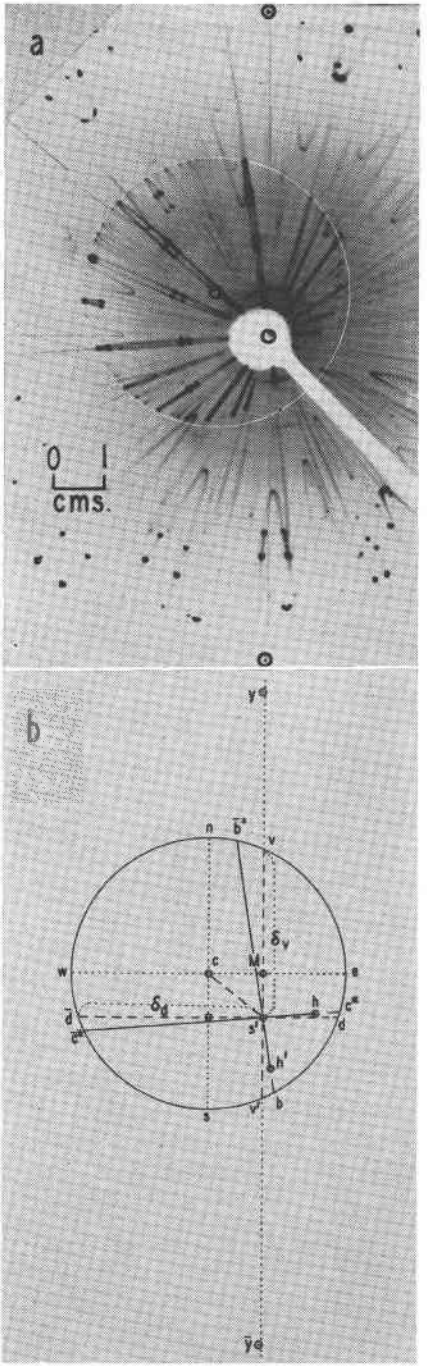

FIG. 30 (*a*) Precession orientation photo of chalcanthite. Same data as Fig. 29, except $\bar{\mu}=10°$ and the orientation is a few degrees out of kilter. (*b*) diagram to explain *a*.

sufficiently pronounced radiating 0-level Laue streaks to indicate that one is dealing with a precessing direction that is either a true crystal axis or some translation direction of the direct lattice whose normal is a plane of the reciprocal lattice which is relatively thickly studded with nodes.

If the orientation shown by this picture is in error, it will more or less resemble Fig. 30*a*, which may be used as an illustrative example.[1a] Working above a light box put scratches along two pronounced streaks nearly at right angles (such as $\bar{c}^*$ and $\bar{b}^*$ of Fig. 30*b*) which establishes the direct beam spot s'. Let the scratch along that streak which it is desired to make parallel to the dial axis ($\bar{c}^*$ in Fig. 30*b*) extend to the edges of the film. If the circle of precession is not well marked (due to a short exposure), its outline may be indicated by a few India ink dots. It should be noted that unless the orientation error is quite small, the radial streaks whose ends mark the circle of precession will be shortened on the direct beam side of the center of the circle of precession. Thus h and h' of Fig. 30*b* mark the end points of certain Laue streaks. Place the film above a light box topped with a glass positive made from metric polar coordinate paper.[2] The center of the circle of precession c is made to coincide with the center of the net, and this is marked by a needle prick. Now with s' above the center of the net, make a scratch through it above the vertical axis of the net when the latter is parallel to a line through the two cassette dots y and $\bar{y}$.[3] Also scratch a line through s' above the dial (horizontal) axis of the net. Scratch the circle of precession, establishing d and $\bar{d}$ on the dial axis, and v and v' on the vertical scratch. Use is made of only one d and one v point; the ones farther from s'. Measure (in mm.) $\delta_v = s'v$ and $\delta_d = s'\bar{d}$. Measure angle $\bar{d}s'\bar{c}^*$ (using the polar net). From the graph (Fig. 31) it is seen that for $\bar{\mu} = 10°$ the value of δ_v ($= 31.3$ mm.) corresponds to a dial error of $4.°78 = 4°47'$. This graph also shows that δ_d ($= 34.1$ mm.) corresponds to an error of $5.°95$ along a "horizontal" arc (one the plane of which is parallel the x-ray beam) of the goniometer head. The angle $\bar{d}s'\bar{c}^*$ ($= 4\frac{1}{4}°$) measures the approximate error along a

[1a] Having obtained such a picture, unless one of the arcs of the goniometer head would be approximately parallel the direct beam when the dial is set correctly, it is often time-saving to take another picture before proceeding further. In doing this, first set the dial to the approximately correct reading; then loosen the set-screw that holds the brass rod (which supports the crystal) in the goniometer head. Now holding this rod tightly with a pair of tweezers, rotate the dial until one of the arcs is parallel the direct beam collimator.

[2] If the film is put on this light box after it has been in the fixer for only a few seconds, the radii and circles of the polar net will be imprinted on it.

[3] On more recent cassettes the two dots mark the dial axis. In this case scratch the horizontal line first, running it through s' parallel to a line through the two dots. The vertical line joining the two cassette dots in Fig. 30 could be made to run through s' by moving the cassette 0.4 mm. to the right along its horizontal axis.

"vertical" arc (one the plane of which is normal to the x-ray beam). These corrections are to be applied as shown in Table 11.

Angle $\bar{d}s'\bar{c}^*$ measured as $4\frac{1}{4}°$ from the film of Fig. 30 is always less than the true angle needed to correct the "vertical" arc, as long as the axis of the cone of precession (marked by c) does not coincide with the direct beam (shown by s'). It is desired that the direction marked by c (Fig. 30) be made to lie at s' and the direction $\bar{c}^*s'$ be made the dial axis. We may think of moving c to M by adjusting the "horizontal" arc and then from M to s' by adjusting the dial. Then the "revised" direction

TABLE 11. INTERPRETATION OF FIG. 30

	Setting when the film was taken	Corrections (ϵ values)	New setting	Correct setting[6]
Dial	291°08	4°47′	286°21′	286°18′
S arc[4]	6.°22l[5]	5.°95(cos 7°) − factor 13.0% = 5.°14	1.°08l	1.°13l
L arc	0.°01l	$4\frac{1}{4}$°(cos 7°) + factor 16.8% = 4.°93	4.°94l	4.°97l

[4] The plane of the S (small) arc is parallel to the direct beam when the dial reads $298\frac{1}{2}°$ (that is, about 7° off the setting used).

[5] l (left) or r (right) are recorded while looking from the crystal towards the goniometer head (Fisher, 1951, 125).

[6] Correct setting (for precession on [a] with [c^*] as the dial axis) determined by methods described ahead.

$\bar{c}^*s'$ is made the dial axis by adjusting the "vertical" arc. Instead of trying to compute these corrections exactly, it is more practical to adjust the "vertical" arc reading by a *positive* percentage factor. Since the radius of the circle of precession of Fig. 30 is 25.4 mm. which corresponds to an error ϵ of 8.°4 (see graph, Fig. 32), one may use *twice* this value as a rough percentage factor of *increase* as shown in Table 11.

In similar fashion the correction obtained for the "horizontal" arc from the δ_d value leads to a high result (for reasons brought out later), and it is practical to adjust this by a *negative* percentage factor of *twice* the arc value of cM[$=8.°4 \sin 51° (=\text{angle } cs'M) = 6.°5$]. It can be seen from the last column of Table 11 that these correction values are adjusted by percentage factors that are somewhat too small. This is immaterial, since it is impossible to get an exactly correct setting from a single picture; the results obtained by the method described are satisfactory for proceeding with the next step in the orientation process.

Using the "new setting" values of Table 11, take a picture which is a double exposure with dial values 180° apart. The two exposures may be differentiated by giving one of them but half the exposure time of the

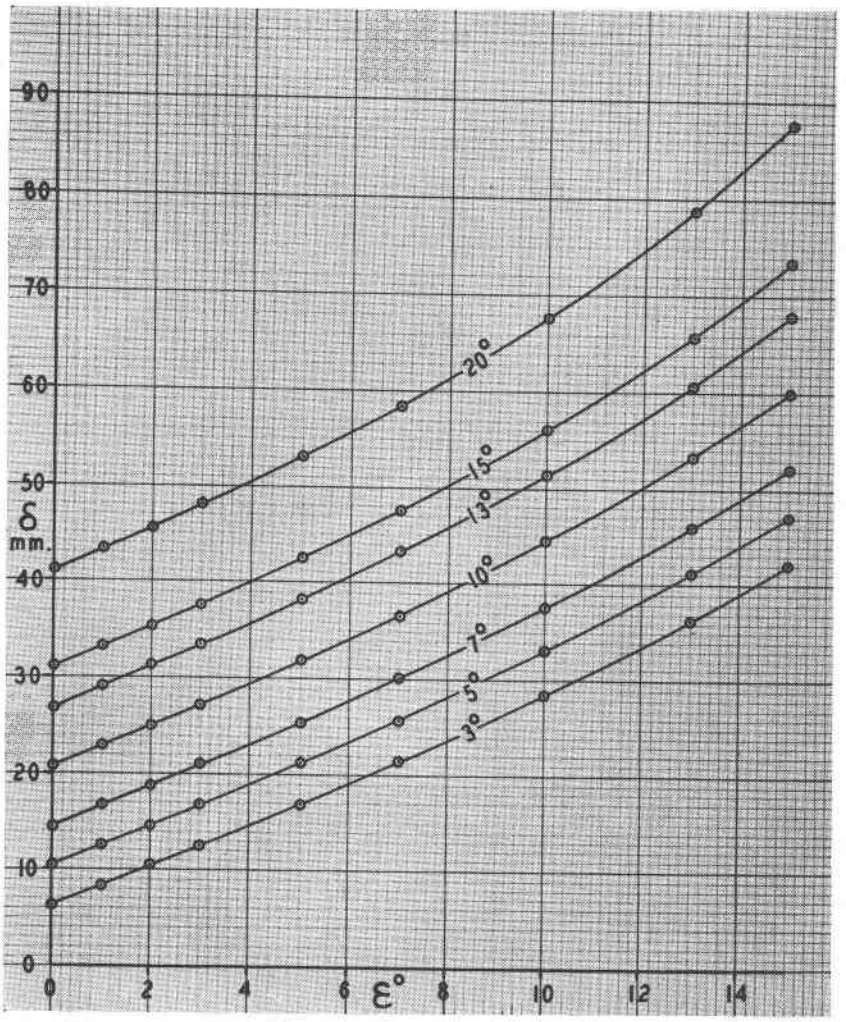

FIG. 31. Graph showing variation in δ (in mm.) with ϵ (in degrees) for various values of $\bar{\mu}$ (the figures on the curves) where $F=60.00$ mm.

other, but it is quicker to keep the times the same and vary the $\bar{\mu}$ value. Moreover since the orientation will be nearly correct, it simplifies things to add the layer-line screen. This amounts to taking ordinary 0-level precession pictures with unfiltered radiation. Since such pictures cannot be taken[6a] on the ordinary precession camera with $\bar{\mu}$ less than 20°,

[6a] Unless one has a layer-line screen with an opening of $r<15$ mm. Thus with an $r=7$ mm. screen, such pictures could be taken with $\bar{\mu}=15°$ ($s=26.1$ mm.), 13° ($s=30.3$ mm.), or 10° ($s=39.7$ mm.).

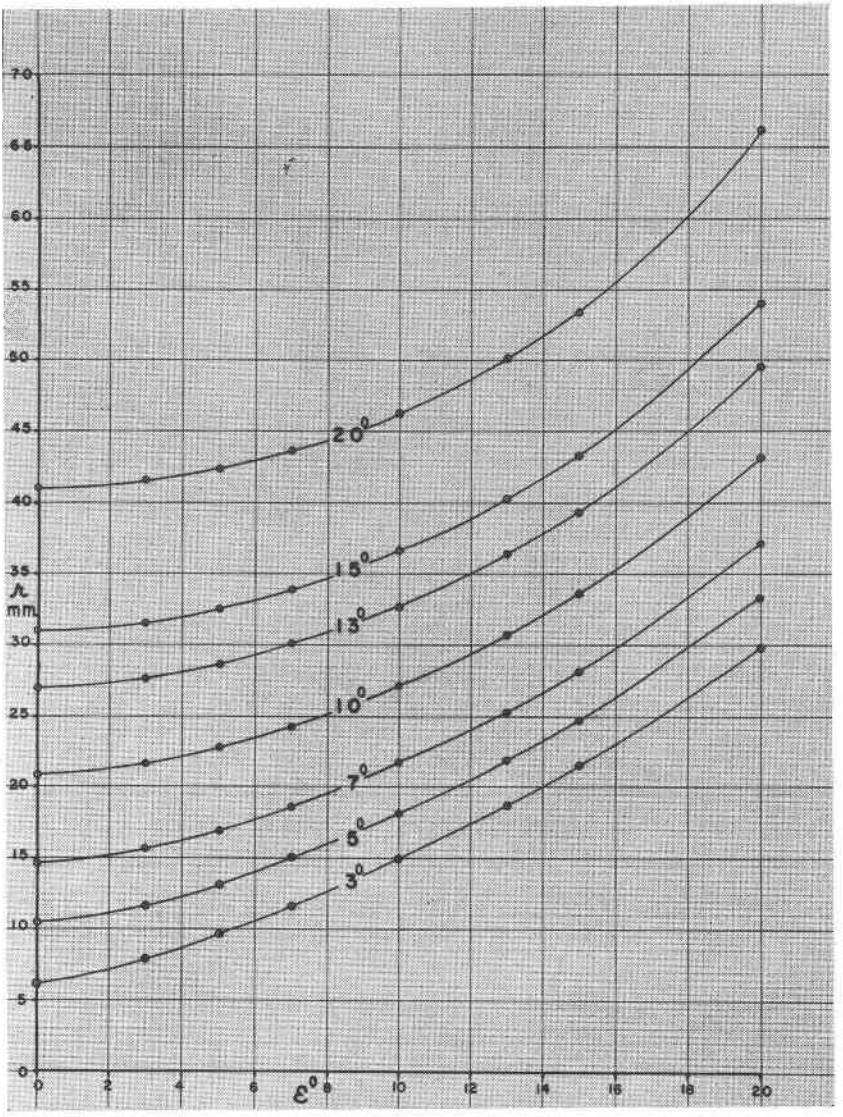

FIG. 32. Graph showing variation in r (in mm.) with ϵ (in degrees) for various values of $\bar{\mu}$ (the figures on the curves) where $F=60.00$ mm.

it is expedient to use precessing angles of 20° and 25°. Such large angles are perhaps unusual for orientation work, but nevertheless they are desirable in the final steps of the orientation procedure to insure satisfactory accuracy.

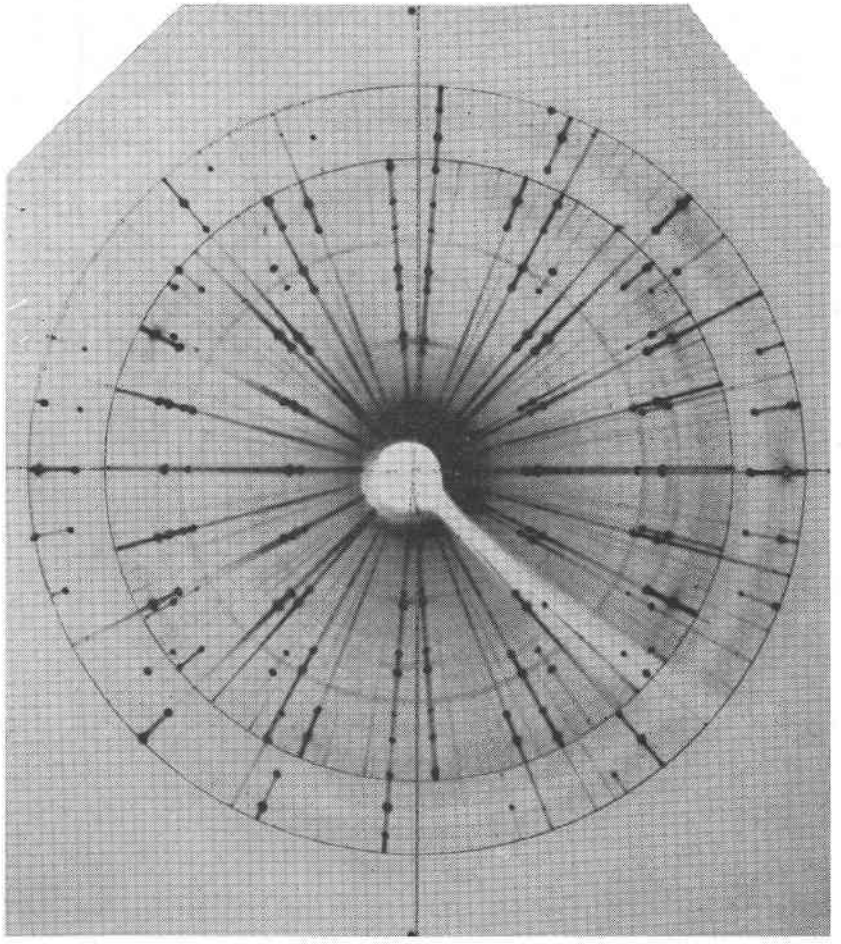

FIG. 33. Precession orientation photo of chalcanthite. Same data as Fig. 29 except a double exposure (with $\bar{\mu}$ values of 20° and 25° at dial readings 180° apart) and a 0-level layer line screen added.

Figure 33 is such a photograph, which may be interpreted as follows. Locate the direct beam spot s' by suitable scratches; the one which marks the dial axis should extend to the right and left edges of the film, using a mean position of the two dial-axis streaks. Place the film above the polar net and establish the centers (c and C) of the two circles of precession; also make a vertical scratch normal to the dial axis going through the mean position of these centers (if c and C are not practically together, scratch ticks along vertical lines through both of them) which intersects the proper circle of precession at n & s for the smaller circle and N & S

for the larger circle. Now scratch the two circles of precession; inspect these under a hand lens to make sure they go exactly through the ends of the streaks; if they do not, make suitable allowances in the following measurements.

The error ϵ (in minutes) of the dial axis reading is found by measuring the difference g or G (in mm.) between the length of $c'\ n$ & $c'\ s$ and of $C'N$ & $C'S$, whence:

$$60g/4.494 = \epsilon \quad (\text{where } \bar{\mu} = 20°) \tag{49}$$

$$60G/4.625 = \epsilon \quad (\text{where } \bar{\mu} = 25°). \tag{50}$$

The denominators of these equations represent the difference in north-south streak lengths (in mm.) for dial orientation errors of 1° at the $\bar{\mu}$ values given (as is shown in Table 12).

The correct "horizontal" arc setting for a camera in perfect adjustment may be obtained from the difference in lengths between values of $s'c'$ and $s'C'$ (c' and C' are points on the dial axis scratch where it is cut by vertical scratches through c and C.). Since in Fig. 33 c' and C' are both to the right of s', it is clear that if the crystal setting were perfect, c' and C' would coincide (they would also coincide with c and C if the dial readings were just right) at a point 0.8 mm. to the right[7] of s'. Call this point O', the center of precession for the film. If the points where the dial axis scratch cuts the circles of precession be designated d (right side) and $\bar{d}$ (left side), where $\bar{\mu}=20°$, and D and $\overline{D}$ (where $\bar{\mu}=25°$), then the difference j or J (in mm.) between the length of $O'd$ & $O'\bar{d}$ and of $O'D$ & $O'\overline{D}$ supplies the error ϵ (in degrees) in the arc settings according to the following formulae:

$$j \cos I/4.494 = \epsilon \quad (\text{where } \bar{\mu} = 20°) \tag{51}$$

$$J \cos I/4.625 = \epsilon \quad (\text{where } \bar{\mu} = 25°) \tag{52}$$

where I is the angle between the plane of the "horizontal" arc and the direct x-ray beam.

It is not satisfactory to get the correction for the "vertical" arc setting by attempting to measure the angle between the two dial streaks of Fig. 33. Instead rotate on the dial axis until another crystal axis is in precessing position; now the other arc of the goniometer head is more or less "horizontal" and another double exposure picture may be taken. From this the desired angle of correction may be computed by the method just outlined.

[7] For perfect adjustment a precession camera must have its dial axis normal to and intersecting V_{vl} (the "vertical" axis through the crystal; see Fig. 6 on page 100 of Fisher 1952 *a*). Their point of intersection 0 is the center of precession for the crystal. Also the cassette holder must have its horizontal axis normal to and intersecting V_{ca} (the "vertical" axis of the cassette); their point of intersection 0′ is the center of precession for the film. And lastly the direct x-ray beam should cut both 0 and 0′!

Explanation of the Two Charts

The graphs of Figs. 31 and 32 are based on data given in Table 12. The derivation of these data may be explained in terms of a special case, Fig. 34*a*. It will be noted that all three orientation circles of precession indicated here have a common chord; namely, the direction which marks

Table 12. Values of δ, D, and r in mm. and of τ in $^{\circ\prime}$ where $F=60.00$ mm. for Various Values of $\bar{\mu}$ and ϵ

$\bar{\mu}$ \ ϵ		0°	1°	2°	3°	5°	7°	10°	13°	15°	20°
3°	δ	6.28	8.39	10.50	12.63	16.97	21.46	28.57	36.35	42.05	59.02
	τ	45-00	36-50	30-54	26-26	20-18	16-19	12-24	9-48	8-30	6-05
	D	—	4.20	8.42	12.63	—	—	—	—	—	—
	r	6.28	6.55	7.13	7.88	9.65	11.65	14.98	18.73	21.50	29.84
5°	δ	10.46	12.57	14.70	16.87	21.25	25.81	33.10	41.14	47.08	65.00
	τ	45-00	39-46	35-26	31-48	26-13	22-04	17-32	14-16	12-32	9-08
	D	—	4.21	8.42	12.68	21.25	—	—	—	—	—
	r	10.46	10.64	11.07	11.68	13.20	15.02	18.20	21.90	24.70	33.34
7°	δ	14.62	16.74	18.89	21.06	25.52	30.17	37.76	45.99	52.19	71.18
	τ	45-00	41-08	37-45	34-37	29-49	25-52	21-10	17-39	15-39	11-37
	D	—	4.22	8.46	12.71	21.33	30.17	—	—	—	—
	r	14.62	14.76	15.11	15.61	16.95	18.63	21.71	25.32	28.14	37.09
10°	δ	20.84	22.98	25.15	27.36	31.93	36.73	44.53	53.35	60.00	80.84
	τ	45-00	42-12	39-39	37-18	33-08	29-34	25-05	21-20	19-09	14-27
	D	—	4.26	8.52	12.81	21.51	30.44	44.53	—	—	—
	r	20.84	20.94	21.21	21.61	22.76	24.28	27.14	30.74	33.62	43.10
13°	δ	26.99	29.16	31.37	33.66	38.31	43.29	51.46	60.84	68.01	91.08
	τ	45-00	42-47	40-43	38-44	35-10	31-57	27-41	23-56	21-39	16-31
	D	—	4.30	8.61	12.98	21.75	30.81	45.14	60.84	—	—
	r	26.99	27.07	27.30	27.65	28.66	30.06	32.81	36.41	39.36	49.54
15°	δ	31.06	33.25	35.49	37.78	42.55	47.66	56.11	65.91	73.48	98.30
	τ	45-00	43-03	41-12	39-26	36-07	33-06	28-58	25-14	22-55	17-32
	D	—	4.34	8.69	13.07	21.96	31.12	45.65	61.64	73.48	—
	r	31.06	31.13	31.33	31.66	32.61	33.95	36.65	40.27	43.31	54.06
20°	δ	41.04	43.33	45.62	48.02	53.07	58.55	67.83	78.91	87.71	118.16
	τ	45-00	43-27	41-58	40-31	37-43	35-02	31-11	27-29	25-05	19-09
	D	—	4.49	8.94	13.44	22.61	32.11	47.31	64.31	77.14	118.16
	r	41.04	41.10	41.27	41.55	42.41	43.66	46.33	50.13	53.46	66.21

Following are $\delta=r$ values where $\epsilon=0°$ for various values of $\bar{\mu}$ not given above:

$\bar{\mu}$	δ or r	$\bar{\mu}$	δ or r	$\bar{\mu}$	δ or r	$\bar{\mu}$	δ or r
4°	8.40	9°	18.77	14°	29.03	18°	37.08
6°	12.54	11°	22.90	16°	33.08	19°	39.07
8°	16.70	12°	24.95	17°	35.08	25°	50.71

For $\bar{\mu}=25°$ and $\epsilon=1°$ have; $\delta=53.06$; $\tau=43°42'$; $D=4.63$; and $r=50.77$.

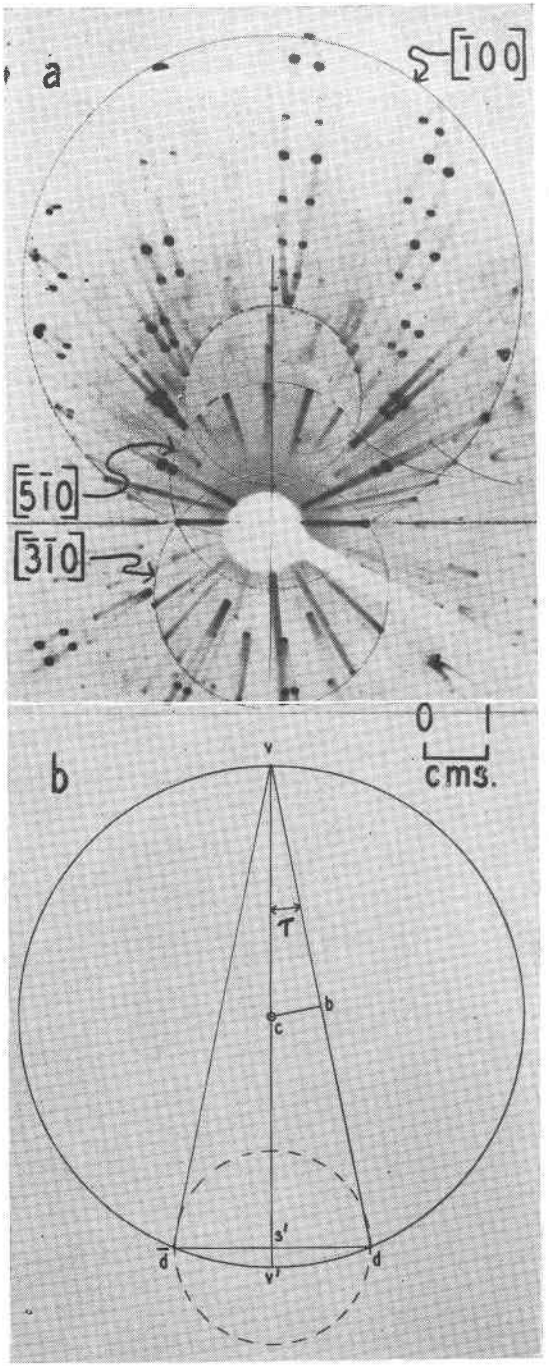

FIG. 34*a*. Precession orientation photo of chalcanthite. Same data as Fig. 29 except the precessing direction is 20°32′ off [*ā*] about the dial axis. Circles of precession are indicated for three zone axes. (*b*) Diagram based on the [1̄00] circle of precession of *a*.

the dial axis. This chord has a length of 29.25 mm., the diameter of a correctly oriented $\bar{\mu}=7°$ circle of precession (see Table 12). Thus as these circles of precession get farther and farther off the correct orientation [that where the center of any given circle coincides with s' (Fig. 34*b*) which represents the precessing direction], they get larger and larger. The method of indexing these circles of precession is given in the next section. The orientation error ϵ of any one of them may be determined from its radius r by using Fig. 32.

A diagram showing the geometry of the largest circle of precession of Fig. 34*a* appears as Fig. 34*b*. Here let $s'd=r_0$, the radius of a correctly oriented ($\epsilon=0°$) circle of precession (in this case where $\bar{\mu}=7°$). Of course

$$r_0 = 2F \sin \bar{\mu} \tag{53}$$

as is evident from Fig. 14 of the previous paper. Buerger [1944, p. 25, (23) and 23′)] gives:

$$\Delta = \frac{\sin 2\epsilon}{\cos (2\epsilon + \bar{\mu})} \quad \text{and} \quad \Delta' = \frac{\sin 2\epsilon}{\cos (2\epsilon - \bar{\mu})}.$$

In the terminology of this paper,

$$\delta = r_0 + F\Delta \qquad (54) \qquad \text{and} \qquad \delta' = r_0 - F\Delta' \qquad (54');$$

where δ' represents the shorter streak ($s'v'$ of Fig. 30*b*), just as δ stands for the longer streak ($s'v$ of Fig. 30*b*). Thus one can compute δ, δ', and also:

$$D = \delta - \delta' = F\Delta + F\Delta' \tag{55}$$

where D is the difference in length of the north & south streaks. It is clear from Fig. 34*b* that

$$\tan \tau = r_0/\delta \tag{56}$$

where $\tau = \angle s'vd$ and $\delta = s'v$. Similarly the radius r of an incorrectly oriented circle of precession is given by (57) or (58). Note in Fig. 34*b* that $r=cv$; and since cb is normal to vd, it follows that $vb=bd$.

$$r = (2vb)/(2 \cos \tau).$$

But

$$vd = \delta/\cos \tau.$$

Thus

$$r = \delta/(2 \cos^2 \tau). \tag{57}$$

Substituting in here the value of δ from (56) gives:

$$r = r_0/\sin 2\tau. \tag{58}$$

The data of Table 12 were computed from these equations.

In Fig. 35 are shown the central portions of two precession orientation photos taken under identical conditions, except in the case of (*b*) the film was 2.00 cms. closer to the crystal than was true for (*a*). Fig. 35*b*

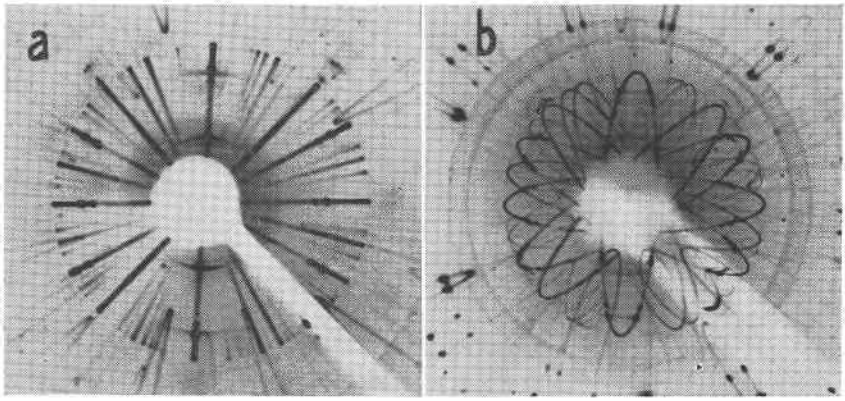

FIG. 35. Precession orientation photos of chalcanthite, precessing on $[\bar{a}]$ with $\bar{\mu}=10°$. (*a*) $F=6.00$ cms. (*b*) Same, except film cassette moved 2.00 cms. closer to the crystal.

is of minor interest, since it shows that where the center of the film is off the center of the second universal joint, the Laue streaks [which are straight lines in (*a*)] split apart into parentheses-like forms. Of course the circle of precession is smaller in (*b*) than in (*a*).

IDENTIFYING NON-AXIAL PRECESSING DIRECTIONS

Non-axial precessing directions can be identified readily by graphical means. Prepare a cross-section of the reciprocal lattice network through its origin and normal to the dial axis. If the dial axis is a reciprocal axis (which is generally the case), the network consists of lines making an interaxial angle (α, β, or γ) with each other. The apparent translations of such a network may be obtained from equations (59) to (70). These are derived from equations like those given in an earlier paper [Fisher 1952*a*, (30) to (35)]. Figure 36[8] shows such a network for chalcanthite with dial axis $[c^*]$. Here $\gamma=77°26'$, $G=0.884$, and $J=1.553$ cms.; note that G & J are defined in (59) & (63) below. Then $[\bar{1}\bar{1}0]$ is normal to a line through the origin and the point marked $(\bar{1}10)$; $[\bar{3}\bar{1}0]$ is normal to a central line through the point marked $(\bar{1}30)$, etc. The directional indices may be obtained by cross-multiplication, the standard zonal procedure, providing one first replaces the nought of the final digit of the index by unity. From the graph an ordinary protractor suffices to measure the angle between the non-axial precessing direction (such as $[\bar{1}\bar{1}0]$ or $[\bar{3}\bar{1}0]$) and $[\bar{a}]$ or $[\bar{b}]$, and thus its identification is readily accomplished.

[8] This diagram has $-[c^*]$ at the center because it was prepared to illustrate an actual working case looking from the dial towards the crystal, and it was assumed that $+[c^*]$ in the crystal extended from the mounted end of the crystal *away from* the goniometer head.

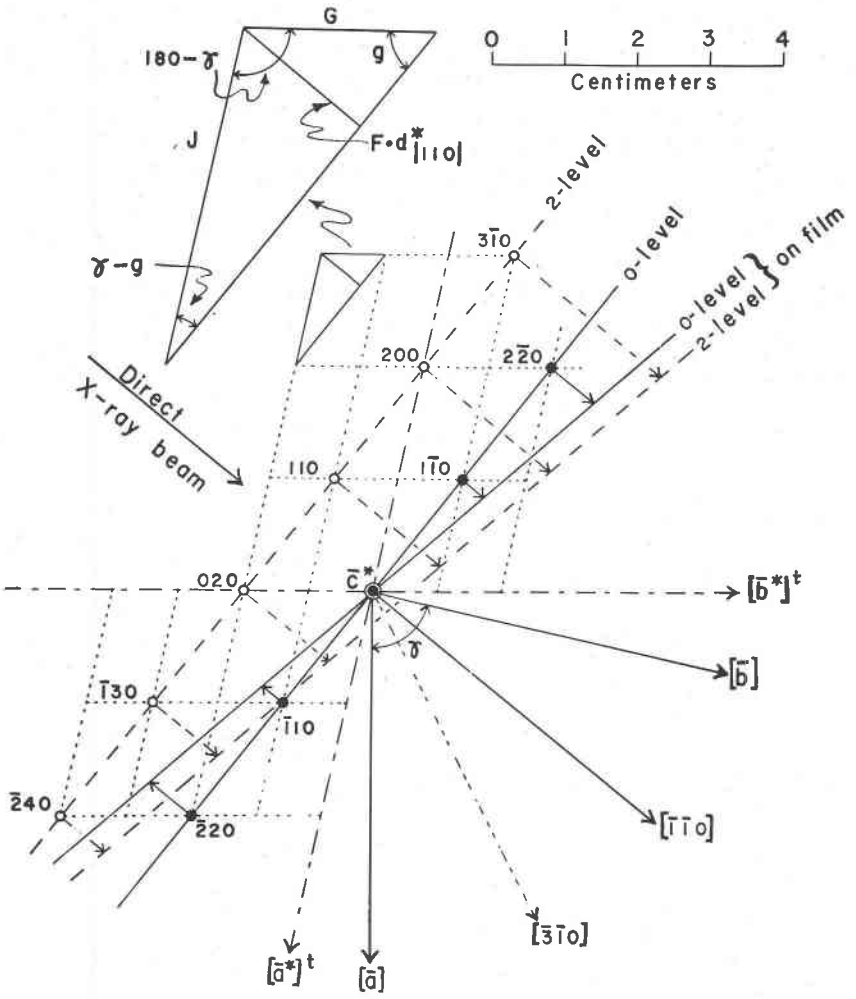

FIG. 36. Cross-section of the reciprocal lattice network of chalcanthite normal to [c^*] on a scale to fit copper radiation at $F=60.00$ mm. Note that no nodes of the reciprocal lattice (except the one at its origin) lie in the plane of this cross-section.

An example is shown in Fig. 34.

Precession on [a]

$G = b^* \sin \alpha^* F\lambda$ (59) where $G = t^*_{\perp c^*}$ and D (dial axis) $= c^*$

$G = F\lambda/(b \sin \gamma)$ (60)

$H = c^* \sin \alpha^* F\lambda$ (61) where $H = t^*_{\perp b^*}$ and $D = b^*$

$H = F\lambda/(c \sin \beta)$ (62)

Precession on $[b]$

$$J = a^* \sin \beta^* F\lambda \quad (63) \qquad \text{where} \quad J = t^*{}_{\perp c^*} \quad \text{and} \quad D = c$$

$$J = F\lambda/(a \sin \gamma) \quad (64)$$

$$K = c^* \sin \beta^* F\lambda \quad (65) \qquad \text{where} \quad K = t^*{}_{\perp a^*} \quad \text{and} \quad D = a^*$$

$$K = F\lambda/(c \sin \alpha) \quad (66)$$

Precession on $[c]$

$$M = a^* \sin \gamma^* F\lambda \quad (67) \qquad \text{where} \quad M = t^*{}_{\perp b^*} \quad \text{and} \quad D = b^*$$

$$M = F\lambda/(a \sin \beta) \quad (68)$$

$$N = b^* \sin \gamma^* F\lambda \quad (69) \qquad \text{where} \quad N = t^*{}_{\perp a^*} \quad \text{and} \quad D = a^*$$

$$N = F\lambda/(b \sin \alpha) \quad (70)$$

From the above one can derive:

$$G \sin \gamma = N \sin \alpha; \qquad G \sin \gamma^* = N \sin \alpha^*. \quad (71)$$

$$H \sin \beta = K \sin \alpha; \qquad H \sin \beta^* = K \sin \alpha^*. \quad (72)$$

$$J \sin \gamma = M \sin \beta; \qquad J \sin \gamma^* = M \sin \beta^*. \quad (73)$$

Computing Reciprocal Lattice Spacings

Buerger (1942, 365) lists "Conditions B" which he states are essential in choosing a reciprocal cell corresponding to the reduced primitive triclinic cell. These conditions may be stated more simply as follows providing one assumes the $c<a<b$ rule:

$$d^*_{|100|} > d^*_{|010|} > d^*_{|1\bar{1}0|} > d^*_{|110|}$$

$$d^*_{|001|} > d^*_{|100|} > d^*_{|101|} > d^*_{|10\bar{1}|}$$

$$d^*_{|001|} > d^*_{|010|} > d^*_{|011|} > d^*_{|01\bar{1}|}$$

The computation of the necessary reciprocal spacings in directions other than those normal to "reciprocal pinacoidal" planes may be carried out by means of equations (74) to (85). The derivation of these may be illustrated for (82) & (83) by the triply-enlarged "diagonal half-mesh" of the reciprocal lattice shown in the upper left corner of Fig. 36.

Dial axis $[a^*]$

To compute $e = \perp[011] \wedge [c^*]^t$, use the tangent law:

$$\tan\left(e - \frac{\alpha}{2}\right) = \left(\tan \frac{\alpha}{2}\right)\left(\frac{N-K}{N+K}\right) \quad (74)$$

and

$$Fd^*_{|011|} = K \cdot \sin e. \quad (75)$$

To compute $e' = \perp[01\bar{1}] \wedge [c^*]^t$, the tangent law yields;

$$\tan\left(90 - \frac{\alpha}{2} - e'\right) = \tan\left(90 - \frac{\alpha}{2}\right) \cdot \left(\frac{K-N}{K+N}\right) \quad (76)$$

and

$$Fd^*_{|01\bar{1}|} = K \cdot \sin e'. \quad (77)$$

Dial axis $[b^*]$

To compute $f = \perp[101] \wedge [a^*]^t$, use the tangent law:

$$\tan\left(f - \frac{\beta}{2}\right) = \left(\tan\frac{\beta}{2}\right)\left(\frac{H - M}{H + M}\right) \tag{78}$$

and

$$Fd^*_{|101|} = M \cdot \sin f. \tag{79}$$

To compute $f' = \perp[10\bar{1}] \wedge [a^*]^t$, the tangent law gives:

$$\tan\left(90 - \frac{\beta}{2} - f'\right) = \tan\left(90 - \frac{\beta}{2}\right) \cdot \left(\frac{M - H}{M + H}\right) \tag{80}$$

and

$$Fd^*_{|10\bar{1}|} = M \cdot \sin f'. \tag{81}$$

Dial axis $[c^*]$

To compute $g = \perp[110] \wedge [b^*]^t$, use the tangent law:

$$\tan\left(g - \frac{\gamma}{2}\right) = \left(\tan\frac{\gamma}{2}\right)\left(\frac{J - G}{J + G}\right) \tag{82}$$

and

$$Fd^*_{|110|} = G \cdot \sin g. \tag{83}$$

To compute $g' = \perp[1\bar{1}0] \wedge [b^*]^t$, the tangent law yields:

$$\tan\left(90 - \frac{\gamma}{2} - g'\right) = \tan\left(90 - \frac{\gamma}{2}\right) \cdot \left(\frac{G - J}{G + J}\right) \tag{84}$$

and

$$Fd^*_{|1\bar{1}0|} = G \cdot \sin g'. \tag{85}$$

Note. The two sides of equations (74), (80), and (84) turn out to be negative in the case of chalcanthite. Of course they could be put in positive fashion, but it seems better to keep the equation triplets with similar forms, even though the signs may then become negative. The sign can be determined easily from a graphical check of angles e, f, and g.

Indexing Precession Photographs

Precession photos where a crystal axis is the precessing axis are indexed on inspection. This is illustrated in an earlier paper (Fisher, 1952 *a*, Figs. 7 and 8). Where some other direction of precession is chosen, a simple graphical procedure suffices. Thus Fig. 37*a* is a precession picture of chalcanthite (0- and 2-levels on a single film) where $[1\bar{1}0]$ is the precession axis and $[c^*]$ is the dial axis. If a trace-o-film copy of Fig. 37*a* is made and placed *upside down* above Fig. 36 so that $[c^*]$ on the trace-o-film lies above the $[1\bar{1}0]$ direction of Fig. 36, with the (000) points of the two coinciding, it will be found that the spots on the $[1\bar{1}0]^*$ direction of the trace-o-film (for both 0- and 2-levels) will lie above the tips of the arrows shown along these two "film" levels in Fig. 36. Once these spots are indexed, since those along $[c^*]$ may be indexed on inspection, it is simple to index all the spots on the picture (see Fig. 37 *b*). The explanation of this procedure is obvious if one holds the sheet of trace-o-film

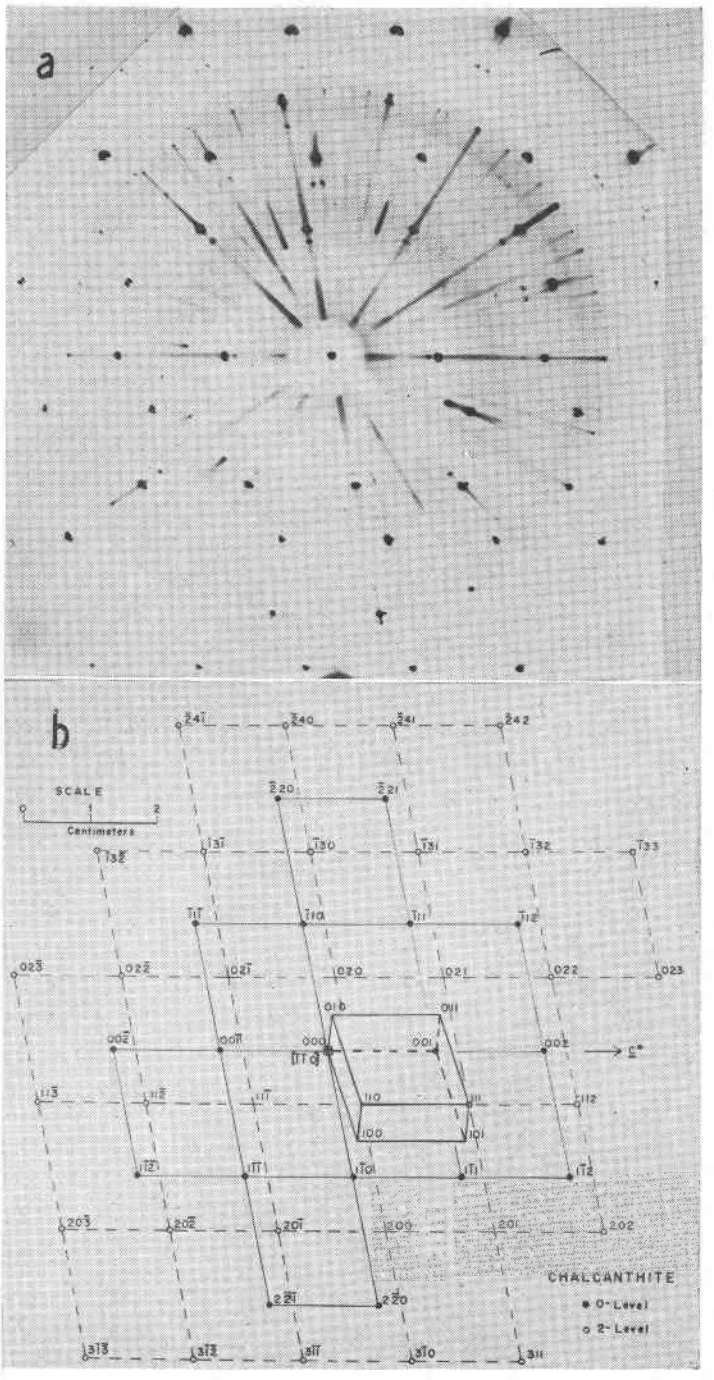

FIG. 37*a*. Precession photo of chalcanthite, 0- and 2-levels, precessing on [$1\bar{1}0$]. $F=6.00$ cms., $\bar{\mu}=20°$, Cu K_α radiation. (*b*) Reciprocal lattice projection to fit *a*.

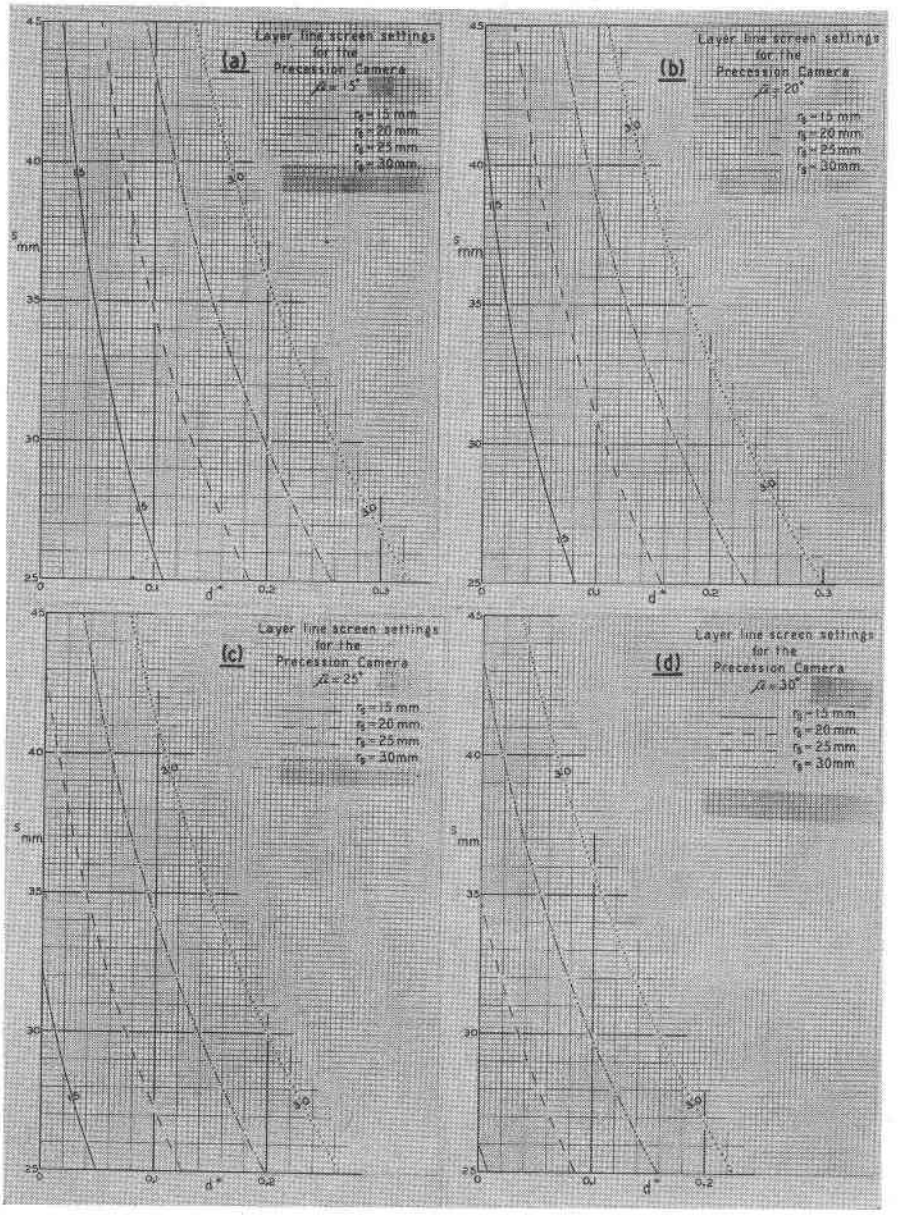

FIG. 38. Charts for determining s-settings of the various layer line screens ($r = 15$, 20, 25, or 30 mm. shown by different types of lines).

(*a*) $\bar{\mu} = 15°$; (*b*) $\bar{\mu} = 20°$; (*c*) $\bar{\mu} = 25°$; (*d*) $\bar{\mu} = 30°$.

above Fig. 36 normal to the arrow marked "Direct X-ray Beam" (with the marked side of the trace-o-film towards this arrow and [c^*] pointing *downwards* at the center of the figure) and imagines the (000) point on the trace-o-film coincides with the center of the figure.

Charts for Setting Layer-Line Screens

In the original publication, Buerger (1944, p. 7) presented a simple graph for setting layer-line screens of $r=15$ and 30 mm. where $\bar{\mu}=20°$. Similar graphs covering screens of $r=15$, 20, 25, & 30 mm. and $\bar{\mu}$-values of 15°, 20°, 25°, & 30° are given in Fig. 38. The writer has these on a single sheet in his laboratory, using different colors for different $\bar{\mu}$-values. Nomograms to accomplish the same end have been published by Evans *et al.* and by Tavora.

References

Buerger, M. J. (1942), *X*-ray crystallography, New York.

——— (1944), The photography of the reciprocal lattice: *Amer. Soc. X-ray & Electron Diffraction, Monogr.* No. **1**, 37 pp.

Evans, H. T., Tilden, S. G., and Adams, P. (1949), New techniques applied to the Buerger precession camera for x-ray diffraction studies: *Rev. Sci. Instr.*, **20**, 155–159.

Fisher, D. J. (1951), Setting a given direction parallel to the axis of a goniometer head: *Am. Mineral.*, **36**, 123–128.

——— (1952*a*), The lattice constants of synthetic chalcanthite, etc. *Ibid.*, **37**, 95–114.

——— (1952*b*), Cone-axis diffraction patterns: *Ibid.*, **37**, 1007–1035.

——— (1952*c*), New universal microscope goniometer: *Ibid.*, **37**, 289 (abstract).

Tavora, E. (1951), A new chart for setting the Buerger precession camera: *Acad. Brasil de Ciencias*, **23**, 113–118.

Manuscript submitted July 23, 1952.